Physics of the Earth and Planetary Interiors, 24 (1981) 325–332
Elsevier Scientific Publishing Company, Amsterdam – Printed in The Netherlands

UPWELLING FLOW IN EARTH'S MANTLE AND SEA-FLOOR SPREADING

LI YINTING (李丽亭) and GUAN DEXIANG (关德相)

Institute of Mechanics, Academia Sinica, Peking (Peoples' Republic of China)

(Received March 12, 1980; accepted for publication July 8, 1980)

Li Yinting and Guan Dexiang, 1981. Upwelling flow in Earth's mantle and sea-floor spreading. Phys. Earth Planet. Inter., 24: 325–332.

Upwelling flows in the Earth's mantle are accompanied by mass, momentum and energy transports from deep to upper layers. Those flows beneath the mid-ocean ridges give rise to sea-floor spreading. Mantle plumes, on the other hand, cause hot spots to be formed on the Earth's surface. Using the basic equations of fluid dynamics, temperature and velocity distributions in two-dimensional upwelling and cylindrical plumes can be obtained by an integral-relation method. Then the mass, momentum and energy transported to the lithosphere by these upwelling flows can readily be calculated. Based on those results we can more thoroughly discuss problems of plate dynamics, such as the driving mechanism of plate motion, the causes of formation of rift valleys over mid-ocean ridges, and the effect of mantle plumes on sea-floor spreading.

1. Introduction

Sea-floor spreading and plate tectonics serve to explain tectonic and seismic activity within the upper layer of the Earth. However, some questions about plate dynamics still remain unsolved.

The causes of plate motion lie in the interior of the Earth. Dynamical processes in the upper layer of the Earth are due to heat- and mass-transfer from the interior. The most efficient manner of heat- and mass-transfer in the mantle is, of course, thermal convection. Although the cell structure of mantle convection is complex and its shape almost unimaginable, there is no doubt that a rising slab exists in each convection cell. This is the upwelling flow of mantle materials. The transfer of mass, momentum and energy from deep to upper layers is carried out by this upwelling flow. It is suggested that the origins of plate motion and the rift valleys over mid-ocean ridges are due to two-dimensional upwelling flows, and the origin of surface hot spots is due to cylindrical plumes.

The mid-ocean ridges are accreting plate margins. There is an upwelling channel (crack) within the lithosphere beneath mid-ocean ridges, through which mantle materials ascend and accrete on the plate margins. These cracks separate the lithosphere into different plates. These cracks form through the long-term melting action of the large heat flux carried by the rising slab of the convection cell. The presence of these cracks, in turn, stabilizes the rising slab of the convection cell beneath mid-ocean ridges. Thus, the system of upwelling flow consists of rising flow in mantle convection cells and flow in channels within the lithosphere beneath mid-ocean ridges. Using fluid dynamical equations, Li Yinting and Guan Dexiang (1979) obtained temperature and velocity distributions in the two-dimensional upwelling flow by the integral-relation method. Based on these results, the mass, momentum and energy transported by the upwelling flow to the lithospheric plate were then calculated. The velocity of the plate motion, the force exerted on the plate by the upwelling flow, and the energy transported by this upwelling flow have also been estimated.

This model of the upwelling flow has also been

used to obtain the topographic profile of the rift valley over the axial part of the mid-ocean ridges (Li Yinting et al., 1979). Calculated results for the depths and widths of the rift valleys agree quantitatively with actual observations. Thus, it is believed that this model may provide a reasonable basis for the study of the dynamics of rift valley formation.

It is essential, both for an understanding of the causes of hot spots on the Earth's surface, and for answering the question of the relation of mantle plumes to sea-floor spreading, that a thorough study is made of ascending flow in cylindrical mantle plumes. Temperature and velocity distributions in mantle plumes and the energy transported by plumes have been obtained by the integral-relation method using the fluid dynamic equation (Guan Dexiang et al., 1979). The results of the calculations showed that the heat flux to the lithosphere from plumes is much larger than that from two-dimensional upwelling flows. Thus, mantle plumes are able to cause the formation of hot spots, not only along the margins of plates but also in their centers.

2. Two-dimensional upwelling flows and the driving mechanisms for sea-floor spreading

2.1. The fluid dynamic equations for two-dimensional upwelling flows

The general fluid dynamic equations govern the flow of the mantle fluids. According to the features of mantle flows, McKenzie et al. (1974) proposed the following set of equations

$$\frac{\partial}{\partial x}\left(\mu\frac{\partial u}{\partial x}\right)+\frac{\partial}{\partial y}\left(\mu\frac{\partial u}{\partial y}\right)+\frac{\partial\mu}{\partial x}\frac{\partial u}{\partial x}+\frac{\partial\mu}{\partial y}\frac{\partial v}{\partial x}-\frac{\partial p}{\partial x}+\rho g\alpha(T-T_a)=0 \quad (1)$$

$$\frac{\partial}{\partial x}\left(\mu\frac{\partial v}{\partial x}\right)+\frac{\partial}{\partial y}\left(\mu\frac{\partial v}{\partial y}\right)+\frac{\partial\mu}{\partial x}\frac{\partial u}{\partial y}+\frac{\partial\mu}{\partial y}\frac{\partial v}{\partial y}-\frac{\partial p}{\partial y}=0 \quad (2)$$

$$u\frac{\partial T}{\partial x}+v\frac{\partial T}{\partial y}=k\left(\frac{\partial^2 T}{\partial x^2}+\frac{\partial^2 T}{\partial y^2}\right) \quad (3)$$

$$\frac{\partial u}{\partial x}+\frac{\partial v}{\partial y}=0 \quad (4)$$

where the symbols used are the same as those used by Li Yinting and Guan Dexiang (1979). The coordinate system is shown in Fig. 1.

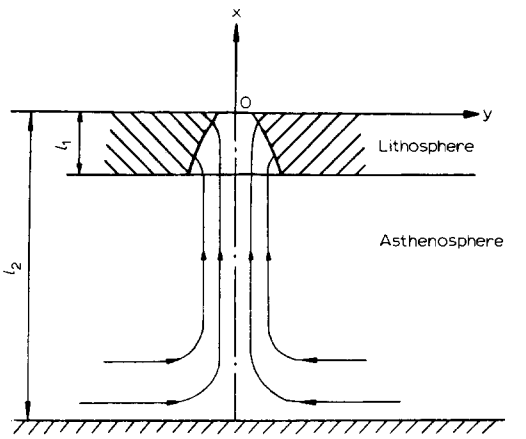

Fig. 1. Sketch of the upwelling flows.

Since both Prandtl number and Rayleigh number are very large for mantle flow, the central portion of the convection cell will remain as a basically stationary nucleus in which the temperature change is small (Turcotte and Oxburgh, 1967). On both sides of a cell are the uprising and downgoing flows, where temperature and velocity change rapidly over short distances. For a convection cell at a depth of 700 km, the horizontal distance over which the dominant changes of temperature and velocity occur ranges from a few to tens of kilometers. The distance over which the dominant changes in the rising velocity occur (i.e. from maximum at the axis of symmetry to zero at the boundary) is defined as the flow thickness of the upwelling flow, denoted by δ_u. The distance over which the change in temperature of the uprising flow occurs (i.e. from the highest temperature at the axis of symmetry to the ambient temperature at the same depth) is defined as the thermal thickness of the upwelling flow, denoted by δ_T. Parameters at $y = 0$ are represented by the subscript w; parameters at both sides of the channel or the outer margins of the uprising flow in the asthenosphere are represented by the subscript a; l_1 is the thickness of the lithosphere and l_2 is the starting depth of the convection. Typical values of u, v, p and μ are represented by U, V, P, M. Typical values of temperature difference in the x- and y-directions are represented by $\Delta_x T$ and $\Delta_y T$, respectively. The characteristic distance in the x-direction is represented by l ($l = l_1$, for the lithosphere, $l =$

$l_2 - l_1$ for the asthenosphere). From $\delta_u^2 << l^2$, it follows that

$$\frac{\partial}{\partial x}\left(\mu \frac{\partial u}{\partial x}\right) << \frac{\partial}{\partial y}\left(\mu \frac{\partial u}{\partial y}\right) \tag{5}$$

$$\frac{\partial}{\partial x}\left(\mu \frac{\partial v}{\partial x}\right) << \frac{\partial}{\partial y}\left(\mu \frac{\partial v}{\partial y}\right) \tag{6}$$

If $\Delta_y T/\Delta_x T >> (\delta_T/l)^2$, then

$$\frac{\partial^2 T}{\partial x^2} << \frac{\partial^2 T}{\partial y^2} \tag{7}$$

From eq. 4, we have

$$\frac{V}{U} \simeq \frac{\delta}{l} \tag{8}$$

so eq. 2 yields

$$P \simeq \frac{\mathrm{M}V}{\delta_u} \tag{9}$$

From eq. 1 and using eqs. 8 and 9, it follows that

$$\frac{P/l}{\mathrm{M}V/\delta_u^2} \simeq \left(\frac{\delta_u}{l}\right)^2 << 1 \tag{10}$$

Thus, in the set of equations (1)–(4), we can neglect the terms

$$\frac{\partial}{\partial x}\left(\mu \frac{\partial u}{\partial x}\right), \frac{\partial}{\partial x}\left(\mu \frac{\partial v}{\partial x}\right), \frac{\partial^2 T}{\partial x^2}, \frac{\partial p}{\partial x}, \frac{\partial \mu}{\partial x}\frac{\partial u}{\partial x}, \frac{\partial \mu}{\partial y}\frac{\partial v}{\partial x}, \text{etc.}$$

Equation 2 does not couple with the rest of the set. Thus we obtain the following set of equations

$$\frac{\partial}{\partial y}\left(\mu \frac{\partial u}{\partial y}\right) + \rho g \alpha (T - T_a) = 0 \tag{11}$$

$$\frac{\partial u}{\partial x} + \frac{\partial v}{\partial y} = 0 \tag{12}$$

$$u \frac{\partial T}{\partial x} + v \frac{\partial T}{\partial y} = k \frac{\partial^2 T}{\partial y^2} \tag{13}$$

2.2. *The solution of the differential equations of the upwelling flow*

By analogy with the Kármán–Pohlhausen single parameter approximate method, we can solve the set of equations (11)–(13) in the following manner. Let

$$\varphi(\eta_u) = \frac{u}{u_w} = a_0 + a_1\eta_u + a_2\eta_u^2 + a_3\eta_u^3 + a_4\eta_u^4 \tag{14}$$

$$\theta(\eta_T) = \frac{T - T_a}{T_w - T_a} = b_0 + b_1\eta_T + b_2\eta_T^2 + b_3\eta_T^3 + b_4\eta_T^4 \tag{15}$$

$$\eta_u = y/\delta_u\,,\ \eta_T = y/\delta_T\,,\ \epsilon = \delta_T/\delta_u \tag{16}$$

where $\delta_T \leqslant \delta_u$. The boundary conditions of eqs. 11–13 become

$$\left.\begin{array}{ll} \varphi = 0 & \text{at } \eta_u = 1 \\ \varphi = 1\,,\ \dfrac{\partial\varphi}{\partial\eta_u} = 0\,,\ \dfrac{\partial^3\varphi}{\partial\eta_u^3} = 0 & \text{at } \eta_u = 0 \\ \theta = 0 & \text{at } \eta_T = 1 \\ \theta = 1\,,\ \dfrac{\partial\theta}{\partial\eta_T} = 0\,,\ \dfrac{\partial^3\theta}{\partial\eta_T^3} = 0 & \text{at } \eta_T = 0 \end{array}\right\} \tag{17}$$

From these conditions we obtain

$$\varphi(\eta_u) = 1 + a_2\eta_u^2 - (1 + a_2)\,\eta_u^4 \tag{18}$$

$$\theta(\eta_T) = 1 + b_2\eta_T^2 - (1 + b_2)\,\eta_T^4 \tag{19}$$

Parmentier and Turcotte (1978) have recently investigated finite amplitude convection in a non-Newtonian fluid and adopted a power-law constitutive relation with power n. They found that the structure of a convection cell is very close to that of fluids with a constant viscosity, when $n \leqslant 3$. Therefore, like other papers relating to mantle convection (Richter, 1973; McKenzie et al., 1974), we study only the constant viscosity case in detail, considering this as a first step to the study of plate dynamics. For the case $\mu = \mu_{(T)}$ (Vetter and Meissner, 1977), the integral-relation method still remains valid, but becomes complicated.

For μ = constant, an analytical solution can be obtained. Substituting eqs. 18 and 19 into eq. 11, comparing the coefficients and using the continuity condition of $\partial u/\partial y$ at the point $y = \delta_T$, it follows that

$$\tfrac{1}{5} - 2\left(1 + \frac{1}{a_2}\right)\epsilon^2 - \tfrac{2}{15}\,b_2 = 0 \tag{20}$$

$$\frac{1}{a_2} + 2\epsilon^2\left(\tfrac{7}{15} + \frac{b_2}{20}\right) = -(\tfrac{8}{5} + \tfrac{4}{15}b_2)\,\epsilon(1 - \epsilon) \tag{21}$$

$$6\left(1 + \frac{1}{a_2}\right) - \frac{1}{\epsilon^2}(2 + b_2) = 0 \tag{22}$$

from which we obtain

$$a_2 = -6/5,\ b_2 = -1,\ \epsilon = 1 \tag{23}$$

So $\delta_u = \delta_T = \delta$, $\eta_u = \eta_T = \eta$, and

$$\delta = \left[\frac{4.8\, k\mu}{\rho g\alpha(-\mathrm{d}T_w/\mathrm{d}x)}\right]^{1/4} \tag{24}$$

$$u_w = \left[\frac{\rho g\alpha\, k}{1.2\mu(-\mathrm{d}T_w/\mathrm{d}x)}\right]^{1/2} (T_w - T_a) \tag{25}$$

Substituting eqs. 12, 18, 19 and 23–25 into eq. 13, and integrating for y over the region $[0, \delta]$, we obtain

$$\begin{cases} ZZ'' - \frac{19}{204} Z'^2 - \frac{170}{204}\beta Z' + \frac{189}{204}\beta^2 - Z\beta' = 0 \\ Z = 0 \text{ at } x = 0 \text{ or } x = -l_2 \end{cases} \tag{26}$$

where single and double primes represent first- and second-order differentiation with respect to x. $Z = T_w - T_a$, $\beta = -\mathrm{d}T_a/\mathrm{d}x$ when T_a is a linear function of x, which is a good approximation in the Earth's mantle. Equation 26 has the following analytical solution

$$\tilde{Z}_1 = \frac{-\tilde{x}_1(\frac{189}{19} + \tilde{\omega})^{9639/988}(1 - \tilde{\omega})^{969/988}}{\frac{204}{19}\int_{-189/19}^{\tilde{\omega}} [(\frac{189}{19} + \tilde{\omega})^{8651/988}(1 - \tilde{\omega})^{-19/988}]\, \mathrm{d}\tilde{\omega}} \tag{27}$$

and

$$\tilde{Z}_2 = \frac{-[\tilde{x}_2 + (l_2/l_1)]\,(\frac{189}{19} + \tilde{\omega})^{9639/988}(1 - \tilde{\omega})^{969/988}}{\frac{204}{19}\int_{1}^{\tilde{\omega}} [(\frac{189}{19} + \tilde{\omega})^{8651/988}(1 - \tilde{\omega})^{-19/988}]\, \mathrm{d}\tilde{\omega}} \tag{28}$$

TABLE I

Physical parameters for Earth's mantle

Parameters	Values used here
Density, ρ	3.3 g cm^{-3}
Thermometric conductivity, k	2×10^{-2} cm^2 s^{-1}
Gravitational acceleration, g	10^3 cm s^{-2}
Coefficient of expansion, α	3.5×10^{-5} °C^{-1}
Thickness of the lithosphere, l_1	100 (or 70) km
Starting depth, l_2	700 km
Total length of the active mid-ocean ridges, L	60 000 km
Specific heat at constant pressure, C_p	0.27 cal g^{-1} °C^{-1}
Viscosity	10^{18}, 10^{19}, 10^{20} poise
β_1	1.5 (or 1.0) °C km^{-1}
β_2	8.0°C km^{-1} (or eq. 36)

TABLE II

Parameters of plate dynamics

μ (poise)	V_p (cm y^{-1})	F_p (dyn cm^{-1})	W_{total} (cal s^{-1})
10^{18}	1.91	0.152×10^{13}	14.61×10^{11}
10^{19}	1.08	0.480×10^{13}	8.22×10^{11}
10^{20}	0.61	1.52×10^{13}	4.62×10^{11}

where $\tilde{x} = x/l_1$, $\tilde{Z}_1 = Z_1/\beta_1 l_1$, $\tilde{Z}_2 = Z_2/\beta_2 l_1$, $\tilde{\omega} = \mathrm{d}\tilde{Z}/\mathrm{d}\tilde{x}$. The parameters in the region $-l_1 \leqslant x \leqslant 0$ are represented by the subscript 1, and the parameters in the region $-l_2 \leqslant x < -l_1$ are represented by the subscript 2.

2.3. Results of calculations and discussion

The parameters for the Earth's mantle adopted in this paper are listed in Table I.

After $T_w(x)$, $u_w(x)$ and $\delta(x)$ are calculated, we can obtain the parameters of the plate dynamics according to the following formulae (Li Yinting and Guan Dexiang, 1979)

$$V_p = 0.64\, u_{w_1}\delta_1/l_1 \tag{29}$$

$$F_p = (\tfrac{2}{15}\rho g\alpha k\mu\beta_1)^{1/2}\, l_1 \int_{-189/19}^{\tilde{\omega}_1} \tilde{Z}_1(1 - \tilde{\omega})^{-3/2}\, \mathrm{d}\tilde{\omega} \tag{30}$$

$$W_{total} = 1.036\, \rho C_p U_{w_1}\delta_1(T_{w_1} - T_{a_1})L \tag{31}$$

The results of these calculations are listed in Table II.

From Table II, we can see an agreement between calculated and observed plate velocities. If $W_{total} = 8.22 \times 10^{11}$ cal s^{-1} for $\mu = 10^{19}$ poise is chosen as the typical value for the energy transported by upwelling material, it is much greater than the lower limit of the energy which must be supplied by any driving mechanism (4.6×10^{10} cal s^{-1}), as pointed out by McKenzie et al. (1974). Since there are no observational data for the driving force, no comparison can be made. Since the plate moves with constant velocity, the total resistance must balance the total driving force. The resistance is primarily viscous. There is no agreement on the calculations of resistance because there is no agreement on the models of mantle flows. Richter (1973) has propounded a model for calculating resistance.

Making use of Richter's results and adopting the data of the present paper, the resistance is found to be 1×10^{13} dyn cm^{-1}. This is of the same order of magnitude as the 0.5×10^{13} dyn cm^{-1} driving force given in Table II. Therefore the following conclusion can be drawn: the mass, momentum and energy transported to a lithospheric plate by deep-mantle material entering the upwelling channel (crack) below a mid-ocean ridge constitute the principal driving factors of sea-floor spreading.

3. Upwelling flow and the rift valleys over the axial parts of mid-ocean ridges

In our opinion the topography of rift valleys of the axial parts of mid-ocean ridges is the surface expression of upwelling flow beneath the ridges. According to the model proposed in the previous section, the flow in the upwelling channel in the lithosphere exerts viscous shear on its wall. This shear is directed upward and is known as a rising force. This force must be balanced by an excessive weight at the same location, which is produced by a rock column of height h. Let y_w be the horizontal distance to the wall of an upwelling channel from the axis of a rift valley. The rising height $h(y_w)$, as a function of y_w, expresses the topographic profile of the rift valley. Then we can define $H = \text{Max}\ \{h(y_w)\}$ as the depth of the rift valley. The maximum width of an upwelling channel within the lithosphere can be defined as the width of the rift valley, denoted by d_f. The extent of the region where the rising force becomes zero is defined as the width of the inner floor of the rift valley, denoted by d_i.

Substituting eqs. 15 and 23 into eq. 11, and integrating for y over the region $[0, \delta]$, we have

$$\tau_\delta = \tfrac{2}{3}\rho g \alpha \delta(x)(T_w - T_a) \tag{32}$$

where τ_δ represents the rising force per unit length in the x-direction. Letting G represent the excess weight per unit length, the relation

$$G\Delta\delta = \tau_\delta \cdot \Delta x\,,\ G = \tau_\delta \left(\frac{d\delta}{dx}\right)^{-1} \tag{33}$$

can be obtained because an increment Δx in the x-direction corresponds to an increment $\Delta\delta$ in the y-direction within the wall of the upwelling channel.

On the other hand, G must be equal to the difference between the weight of a rock column of height h and that of a water column of the same height, because this space was occupied by seawater before the rock was raised. Then

$$G = (\rho - 1)h \tag{34}$$

and the elevation is given by

$$\begin{cases} h = \dfrac{\rho}{\rho - 1}\,\tfrac{2}{3}\,\alpha\delta(x)\left(\dfrac{d\delta}{dx}\right)^{-1}[T_w(x) - T_a(x)] \\ y = \delta(x) \end{cases} \tag{35}$$

This is the topographic profile of the rift valley.

In order to calculate the functions $\delta(x)$ and $T_w(x)$ in eq. 35, we must solve eq. 26 by a numerical method. Using Simon's equation and experimental data (Griggs, 1972; Miyashiro, 1972; Bottinga and Allègre, 1976), the following relation can be obtained

$$\beta(x) = \tfrac{11}{4}\left[(\tfrac{16}{11})^4 - 1\right]\left\{1 + \frac{|x|}{l_1}\left[(\tfrac{16}{11})^4 - 1\right]\right\}^{-3/4}, \quad |x| < [0, l_1] \tag{36}$$

From eqs. 26 and 36, $Z(x) = T_w(x) - T_a(x)$ can be obtained. Using the relation

$$\delta(x) = \left(\frac{4.8k\mu}{\rho g \alpha}\right)^{1/4}(\beta - Z')^{-1/4} \tag{37}$$

and the values of the parameters in Table I, the topographic profile can be obtained. The calculated results and the measured data for the topographic profile are shown in Fig. 2 by broken and solid curves, respectively.

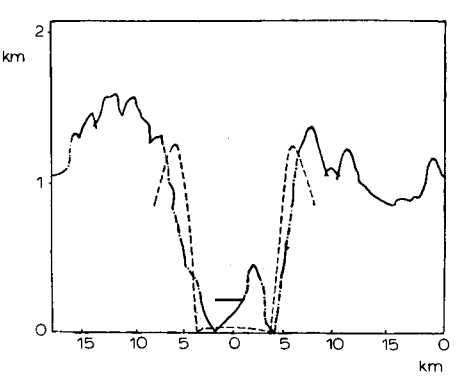

Fig. 2. Topography of rift valley (a comparison between calculated and observed results) (Le Pichon et al., 1973).

TABLE III

Width of the rift valley

Calculated velocity of sea-floor spreading (cm y^{-1})	Width of rift valley (km)	
	Calculated	Observed
2.20	9.2	10
1.24	16.3	
0.69	29.1	30

The results of the calculations for the width of the rift valley are shown in Table III. These results show that the slower the velocity of the sea-floor spreading, the wider the rift valley becomes. This is in agreement with the observations.

The measurement of the inner floor width of the rift valley was made by the "Famous" at the Azores in the Atlantic Ocean (Ballaiche, 1974) where the velocity of sea-floor spreading was found to be 2.3 cm y^{-1} and the inner floor width of the rift valley is 3–5 km. The inner floor width computed in this paper is 3.1 km. The observed depths of the rift valley are known to be 1–2 km, and the result calculated here is 1.26 km for l_1 = 70 km and 1.99 km for l_1 = 100 km.

We must emphasize that there are a variety of factors influencing the topography of rift valleys, and only the rising force exerted on the wall of a channel by upwelling flow was considered here. Therefore the topographic profile computed here might be only a first approximation to the real profile.

4. A fluid-dynamic model of the plume and its effect on geodynamic processes

Recently the phenomenon of "hot spots" on the Earth has attracted the attention of an increasing number of geophysicists (Burke and Wilson, 1976). Some authors have suggested that these hot spots are surface phenomena related to the presence of mantle plume beneath (Morgan, 1971). Although the idea of the mantle plume was proposed many years ago, a reasonable dynamic explanation does not yet exist. Attempts have been made to estimate this ascending flow (Morgan, 1972; Khan, 1973), but a very important process in natural convection, the effect of heat transfer on the motion, was not considered. Guan Dexiang et al. (1979), using the basic fluid-dynamical equations, obtained the extent of the mantle plume, the temperature and velocity of its ascending flow, and the heat transported by the plume to the lithosphere.

We consider this ascending flow in a cylindrical frame. The x-axis is vertically upward and the r- and θ-axes are within the horizontal plane. Then the ascending flow in the plume can be described as an axisymmetric cylindrical flow governed by the following equations

$$\frac{1}{r}\frac{\partial}{\partial r}\left(\mu r \frac{\partial u}{\partial r}\right) + \rho g \alpha (T - T_\infty) = 0 \tag{38}$$

$$u\frac{\partial T}{\partial x} + v\frac{\partial T}{\partial r} = k\frac{1}{r}\frac{\partial}{\partial r}\left(r\frac{\partial T}{\partial r}\right) \tag{39}$$

$$\frac{1}{r}\frac{\partial}{\partial r}(rv) + \frac{\partial u}{\partial x} = 0 \tag{40}$$

where the symbols are the same as those in Guan Dexiang et al. (1979), and μ was assumed constant.

Using the integral-relation method, we can solve the set of equations (38)–(40). Let

$$\varphi = \frac{u}{u_w} = a_0 + a_1\eta_u + a_2\eta_u^2 + a_3\eta_u^3 + a_4\eta_u^4 \tag{41}$$

$$\theta = \frac{T - T_\infty}{T_w - T_\infty} = b_0 + b_1\eta_T + b_2\eta_T^2 + b_3\eta_T^3 + b_4\eta_T^4 \tag{42}$$

where $\eta_u = r/\delta_u$, $\eta_T = r/\delta_T$, $\epsilon = \delta_T/\delta_u$.

The boundary conditions of eqs. 38–40 become

$$\begin{aligned} &\varphi = 0 && \text{when } \eta_u = 1 \\ &\varphi = 1\,,\ \frac{\partial\varphi}{\partial\eta_u} = 0\,,\ \frac{\partial^3\varphi}{\partial\eta_u^3} = 0 && \text{when } \eta_u = 0 \\ &\theta = 0 && \text{when } \eta_T = 1 \\ &\theta = 1\,,\ \frac{\partial\theta}{\partial\eta_T} = 0\,,\ \frac{\partial^3\theta}{\partial\eta_T^3} = 0 && \text{when } \eta_T = 0 \end{aligned} \tag{43}$$

From these conditions, we obtain

$$\varphi(\eta_u) = 1 + a_2\eta_u^2 - (1 + a_2)\eta_u^4 \tag{44}$$

$$\theta(\eta_T) = 1 + b_2\eta_T^2 - (1 + b_2)\eta_T^4 \tag{45}$$

By substituting eqs. 44 and 45 into eq. 38, comparing the coefficients and using the continuity condition of $\partial u/\partial r$ at $r = \delta_T$, we obtain

$$a_2 = -4/3\,,\ b_2 = -1\,,\ \epsilon = 1 \tag{46}$$

Thus $\delta_u = \delta_T = \delta$, $\eta_u = \eta_T = \eta$, and

$$\delta = \left[\frac{64k\mu}{3\rho g\alpha(-\mathrm{d}T_w/\mathrm{d}x)}\right]^{1/4} \tag{47}$$

$$u_w = \left[\frac{3\rho g\alpha k}{4\mu(-\mathrm{d}T_w/\mathrm{d}x)}\right]^{1/2} (T_w - T_\infty) \tag{48}$$

Substituting eqs. 43–48 into eq. 39, and integrating for r over the region $[0, \delta]$, we have

$$\begin{aligned} &68ZZ'' + 87Z'^2 - 206\beta Z' + 119\beta^2 = 0 \\ &Z = 0 \qquad \text{when } x = 0 \text{ or } x = -l \end{aligned} \tag{49}$$

where $Z = T_w - T_\infty$, $\beta = -\mathrm{d}T_\infty/\mathrm{d}x$ = constant. The following analytical solutions can be obtained

$$\tilde{Z} = \frac{(1-\tilde{\omega})^{17/8}[(119/87) - \tilde{\omega}]^{-2023/696}}{\frac{68}{87}\int_{-\infty}^{1} (1-\tilde{\omega})^{783/696}[(119/87) - \tilde{\omega}]^{-2719/696}\,\mathrm{d}\tilde{\omega}} \tag{50}$$

$$\tilde{x} = \frac{-\int_{-\infty}^{\tilde{\omega}} (1-\tilde{\omega})^{783/696}[(119/87) - \tilde{\omega}]^{-2719/696}\,\mathrm{d}\tilde{\omega}}{\int_{-\infty}^{1} (1-\tilde{\omega})^{783/696}[(119/87) - \tilde{\omega}]^{-2719/696}\,\mathrm{d}\tilde{\omega}} \tag{51}$$

where $Z = \beta l\tilde{Z}$, $x = l\tilde{x}$, $\tilde{\omega} = \mathrm{d}\tilde{Z}/\mathrm{d}\tilde{x}$.

From eqs. 50 and 51, we obtain $Z = T_w(x) - T_a(x)$, as shown in Fig. 3. We can see that max $\{T_w(x) - T_\infty(x)\} = 0.5349\,\beta l$, when $|x| = 0.1356\,l$. As $x \to 0$, $\mathrm{d}[T_w(x) - T_\infty(x)]/\mathrm{d}|x| \to \infty$.

Since the temperature change near point $x = 0$ is sharp, the heat transported by the plume to the lithosphere is large. The mantle plume acts like a "hot drill" that steadily drills up to the lithosphere. On drilling through a lithospheric plate, lava overflows in large quantities as volcanic eruptions.

After $T_w(x) - T_\infty(x)$ has been obtained, $\delta(\alpha)$ and $u_w(x)$ can be obtained by using eqs. 47 and 48.

The heat transported by a plume to the lower surface of the lithosphere per unit time, $\dot{Q}$, is the most interesting parameter. Since the point $x = 0$ (i.e. the lower surface of the lithosphere) is a singular point of the solution of the equations governing the ascending flow in a mantle plume, $\dot{Q}$ cannot be obtained from the temperature gradient at this point. Thus, we substitute the section plane at $\tilde{x} = -\epsilon$, where ϵ is very small and positive, for the lower surface of the lithosphere. Using the energy balance relation we obtain

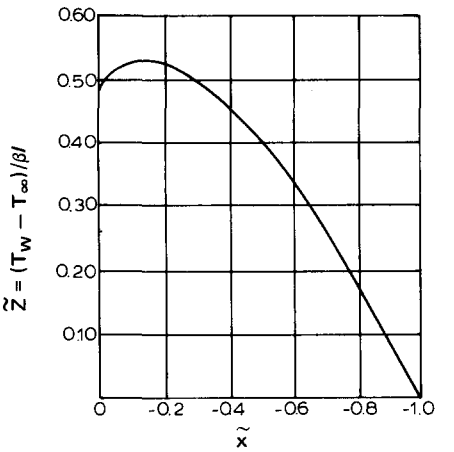

Fig. 3. Dimensionless temperature difference Z plotted versus the dimensional depth.

$$\dot{Q} = \tfrac{11}{9}\,\pi\rho C_p k\beta l^2\,\frac{\tilde{Z}^2}{1-\tilde{\omega}} \tag{52}$$

where $l = 600$ km, $\beta = 1°\mathrm{C\ km^{-1}}$, $\epsilon = 0.01$, $\dot{Q} = 3.7 \times 10^8$ cal s^{-1}. If the number of hot spots in the whole Earth is 122, we obtain $\dot{Q}_{total} = 4.4 \times 10^{10}$ cal s^{-1}. This value is of the same order of magnitude as the energy released by volcanic activity over the whole Earth per second, 1.8×10^{10} cal s^{-1}. Since this $\dot{Q}_{total}$ is much smaller than W_{total}, the energy transported by the upwelling flows beneath the mid-ocean ridges per second, the action of plumes for sea-floor spreading is not as efficient as that of upwelling flows beneath mid-ocean ridges.

5. Concluding remarks

Some geologists and geophysicists have suggested that sea-floor spreading may originate from the penetration of upwelling lava into cracks in the lithosphere. This view remains conjectural, mainly because the upwelling flow cannot be described quantitatively. Using the method of hydrodynamics we have given a mathematical description of the upwelling flow and

have obtained results for the extent of upwelling channels, velocities of plate motion, pushing forces, energy transported to the lithosphere by the upwelling flows, and the topography of the rift valleys over mid-ocean ridges. The results obtained are found to be in good agreement with observational data, indicating that the fluid-dynamical analysis described above is valid.

The results obtained also show that mantle plumes are able to cause the formation of hot spots at the Earth's surface. However, some authors have exaggerated the importance of mantle plumes for sea-floor spreading.

Acknowledgements

The authors are gratefull to Prof. H.S. Tan, Prof. T.H. Yin and Prof. C.Y. Fu for their advice and encouragement.

References

Ballaiche, G., 1974. Inner floor of the rift valley: first submersible study. Nature (London), 250: 558–560.

Bottinga, Y. and Allègre, C., 1976. Geophysical, petrological and geochemical models of the oceanic lithosphere. Tectonophysics, 32: 9–59.

Burke, K.C. and Wilson, J.T., 1976. Hot spots on the Earth's surface. Sci. Am., 235: 46–57.

Griggs, D.T., 1972. The sinking lithosphere and the focal mechanism of deep earthquakes. In: E.C. Robertson (Editor), The Nature of the Solid Earth, McGraw-Hill, New York, NY, pp. 361–384.

Guan Dexiang, Li Yinting and Xue En, 1979. A fluid-dynamic model of the ascending flow in the mantle plume. Sci. Sin., 22: 1070–1081.

Khan, M.A., 1973. Plumes in the mantle. 2nd Int. Symp. Geodesy. Phys. Earth., pp. 363–379.

LePichon, X., Francheteau, J. and Bonnin, J., 1973. Plate Tectonics. Elsevier, Amsterdam.

Li Yinting and Guan Dexiang, 1979. Driving mechanism for sea floor spreading. Sci. Sin., 22: 819–834.

Li Yinting, Guan Dexiang and Xue En, 1979. Dynamical description of the topography of rift valley over axial part of the oceanic ridges. Acta Geophys. Sin., 22: 289–298.

McKenzie, D.P., Roberts, J.M. and Weiss, N.O., 1974. Convection in the Earth's mantle: towards a numerical simulation. J. Fluid Mech., 62: 465–538.

Miyashiro, A., 1972. Pressure and temperature conditions and tectonic significance of regional and ocean-floor metamorphism. Tectonophysics, 13: 141–159.

Morgan, W.J., 1971. Convection plumes in the lower mantle. Nature (London), 230: 42–43.

Morgan, W.J., 1972. Deep mantle convection plume and plate motions. Am. Assoc. Petrol. Geol. Bull., 56: 203–213.

Parmentier, E.M. and Turcotte, D.L., 1978. Studies of finite amplitude non-Newtonian thermal convection with application to convection in the Earth's mantle. J. Fluid Mech., 84: 1–11.

Richter, F.M., 1973. Dynamical models for sea floor spreading. Rev. Geophys. Space Phys., 11 (2): 223–287.

Turcotte, D.L. and Oxburgh, E.R., 1967. Finite amplitude convective cell and continental drift. J. Fluid Mech., 28: 29–42.

Vetter, U.R. and Meissner, R.O., 1977. Creep in geodynamic processes. Tectonophysics, 42: 37–54.